

Time-lapse image registration using the local similarity attribute^a

^aPublished in Geophysics, 74, no. 2, A7-A11, (2009)

Sergey Fomel and Long Jin

ABSTRACT

We present a method for registration of time-lapse seismic images based on the local similarity attribute. We define registration as an automatic point-by-point alignment of time-lapse images. Stretching and squeezing a monitor image and computing its local similarity to the base image allows us to detect an optimal registration even in the presence of significant velocity changes in the overburden. A by-product of this process is an estimate of the ratio of the interval seismic velocities in the reservoir interval. We illustrate the proposed method and demonstrate its effectiveness using both synthetic experiments and real data from the Duri time-lapse experiment in Indonesia.

INTRODUCTION

Time-lapse seismic monitoring is an important technology for enhancing hydrocarbon recovery (Lumley, 2001). At the heart of the method is comparison between repeated seismic images with an attempt to identify changes indicative of fluid movements in the reservoir.

In general, time-lapse image differences contain two distinct effects: shifts of image positions in time caused by changes in seismic velocities and amplitude differences caused by changes in seismic reflectivity. The data processing challenge is to isolate changes in the reservoir itself from changes in the surrounding areas. Cross-equalization is a popular technique for this task (Rickett and Lumley, 2001; Stucchi et al., 2005). A number of different cross-equalization techniques have been successfully applied in recent years to estimate and remove time shifts between time-lapse images (Bertrand et al., 2005; Aarre, 2006). An analogous task exists in medical imaging, where it is known as the *image registration* problem (Modersitzki, 2004).

In this paper, we propose to use the local similarity attribute (Fomel, 2007a) for automatic quantitative estimation and extraction of variable time shifts between time-lapse seismic images. A similar technique has been applied previously to multi-component image registration (Fomel et al., 2005). As a direct quantitative measure of image similarity, local attributes are perfectly suited for measuring nonstationary time-lapse correlations. The extracted time shifts also provide a direct estimate of

the seismic velocity changes in the reservoir. We demonstrate an application of the proposed method with synthetic and real data examples.

THEORY

The correlation coefficient between two data sequences a_t and b_t is defined as

$$c = \frac{\sum_t a_t b_t}{\sqrt{\sum_t a_t^2 \sum_t b_t^2}} \quad (1)$$

and ranges between 1 (perfect correlation) and -1 (perfect correlation of signals with different polarity). The definition of the local similarity attribute (Fomel, 2007a) starts with the observation that the squared correlation coefficient can be represented as the product of two quantities $c^2 = p q$, where

$$p = \frac{\sum_t a_t b_t}{\sum_t b_t^2}$$

is the solution of the least-squares minimization problem

$$\min_p \sum_t (a_t - p b_t)^2, \quad (2)$$

and

$$q = \frac{\sum_t a_t b_t}{\sum_t a_t^2}$$

is the solution of the least-squares minimization

$$\min_q \sum_t (b_t - q a_t)^2. \quad (3)$$

Analogously, the local similarity γ_t is a variable signal defined as the product of two variable signals p_t and q_t that are the solutions of the regularized least-squares problems

$$\min_{p_t} \left(\sum_t (a_t - p_t b_t)^2 + R[p_t] \right), \quad (4)$$

$$\min_{q_t} \left(\sum_t (b_t - q_t a_t)^2 + R[q_t] \right), \quad (5)$$

where R is a regularization operator designed to enforce a desired behavior such as smoothness. Shaping regularization (Fomel, 2007b) provides a particularly convenient method of enforcing smoothness in iterative optimization schemes. If shaping regularization is applied iteratively with Gaussian smoothing as a shaping operator, its

first iteration is equivalent to the fast local cross-correlation method of Hale (2006). Further iterations introduce relative amplitude normalization and compensate for amplitude effects on the local image similarity. Choosing the amount of regularization (smoothness of the shaping operator) affects the results. In practice, we start with strong smoothing and decrease it when the results stop changing and before they become unstable.

The application of local similarity to the time-lapse image registration problem consists of squeezing and stretching the monitor image with respect to the base image while computing the local similarity attribute. Next, we pick the strongest similarity trend from the attribute panel and apply the corresponding shift to the image.

In addition to its use for image registration, the estimated local time shift is a useful attribute by itself. Time shift analysis has been widely applied to infer reservoir compaction (Hatchell and Bourne, 2005; Tura et al., 2005; Janssen et al., 2006; Rickett et al., 2007). Since the time shift has a cumulative effect, it is helpful to compute the derivative of time shift, which can relate the time shift change to the corresponding reservoir layer. Rickett et al. (2007) define the derivative of time shift as *time strain* and find it to be an intuitive attribute for studying reservoir compaction.

What is the exact physical meaning of the warping function $w(t)$ that matches the monitor image $I_1(t)$ with the base image $I_0(t)$ by applying the transformation $I_1[w(t)]$? One can define the base traveltime as an integral in depth, as follows:

$$t = 2 \int_0^{H_0} \frac{dz}{v_0(z)}, \quad (6)$$

where $v_0(z)$ is the base velocity, and H_0 is the base depth. A similar event in the monitor image appears at time

$$w(t) = 2 \int_0^{H_1} \frac{dz}{v_1(z)} = \int_0^{t+\Delta t} \frac{\hat{v}_0(\tau)}{\hat{v}_1(\tau)} d\tau, \quad (7)$$

where H_1 is the monitor depth, $\hat{v}_0(t)$ and $\hat{v}_1(t)$ are seismic velocities as functions of time rather than depth, and Δt is the part of the time shift caused by the reflector movement:

$$\Delta t = 2 \int_{H_0}^{H_1} \frac{dz}{v_1(z)} \quad (8)$$

In a situation where the change of Δt with t can be neglected, a simple differentiation of the function $w(t)$ detected by the local similarity analysis provides an estimate of the local ratio of the velocities:

$$\frac{dw}{dt} \approx \frac{\hat{v}_0(t)}{\hat{v}_1(t)}. \quad (9)$$

If the registration is correct, the estimated velocity ratio outside of the reservoir should be close to one. One can connect the local velocity ratio to other physical attributes that are related to changes in saturation, pore pressure, or compaction.

We demonstrate the proposed procedure in the next section using several examples.

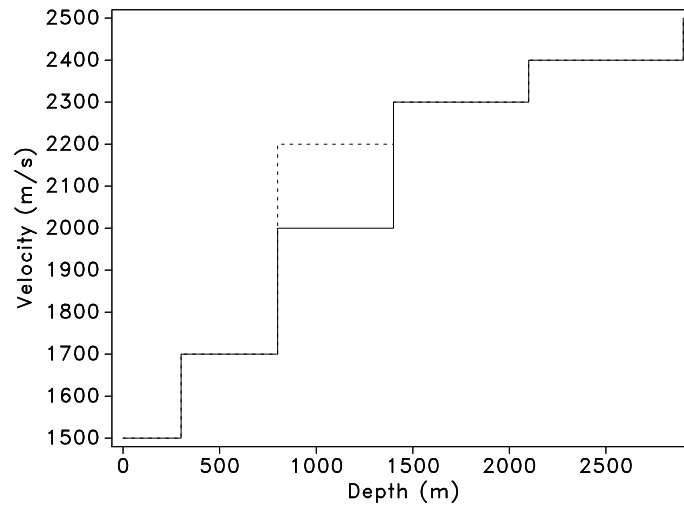
EXAMPLES

1-D synthetic data

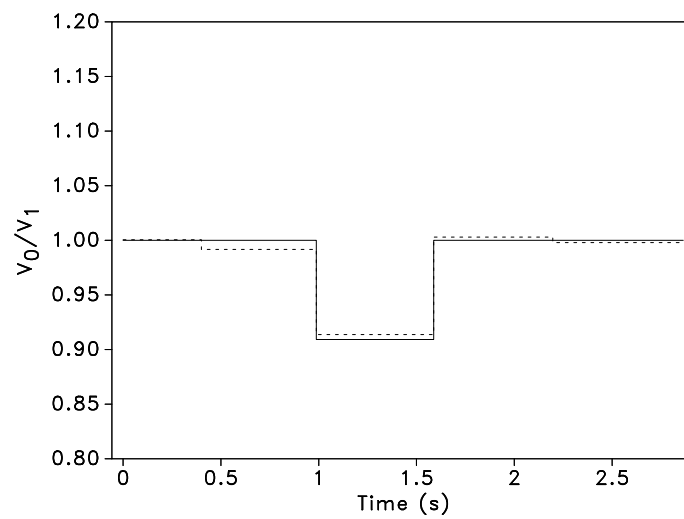
Figure 1(a) shows a simplistic five-layer velocity model, where we introduce a velocity increase in one of the layers to simulate a time-lapse effect. After generating synthetic image traces, we can observe, in Figure 2(a), that the time-lapse difference contains changes not only at the reservoir itself but also at interfaces below the reservoir. Additionally, the image amplitude and the wavelet shape at the reservoir bottom are incorrect. These artifact differences are caused by time shifts resulting from the velocity change. After detecting the warping function $w(t)$ from the local similarity scan, shown in Figure 3, and applying it to the time-lapse image, the difference correctly identifies changes in reflectivity only at the top and the bottom of the producing reservoir [Figure 2(b)]. To implement the local similarity scan, we use the *relative stretch* measure $s(t) = w(t)/t$. When the two images are perfectly aligned, $s(t) = 1$. Deviations of $s(t)$ from one indicate possible misalignment. Finally, we apply equation 9 to estimate interval velocity changes in the reservoir and observe a reasonably good match with the exact synthetic model [Figure 1(b)].

2-D synthetic data

Figure 4(a) shows a more complicated 2-D synthetic example. In this experiment, we assume that the changes occur both in the reservoir and in the shallow subsurface [Figure 4(b)]. The synthetic data were generated by convolution modeling. After computing local similarity between the two synthetic time-lapse images [Figure 5], we apply the extracted stretch factor to register the images. Figures 4(c) and 4(d) compare time-lapse difference images before and after registration. Similarity-based registration effectively removes artifact differences both above and below the synthetic reservoir. As mentioned before, the local similarity cube is an important attribute by itself and includes information on uncertainty bounds for the local stretch factor, which reflects the uncertainty of the reservoir parameter estimation.

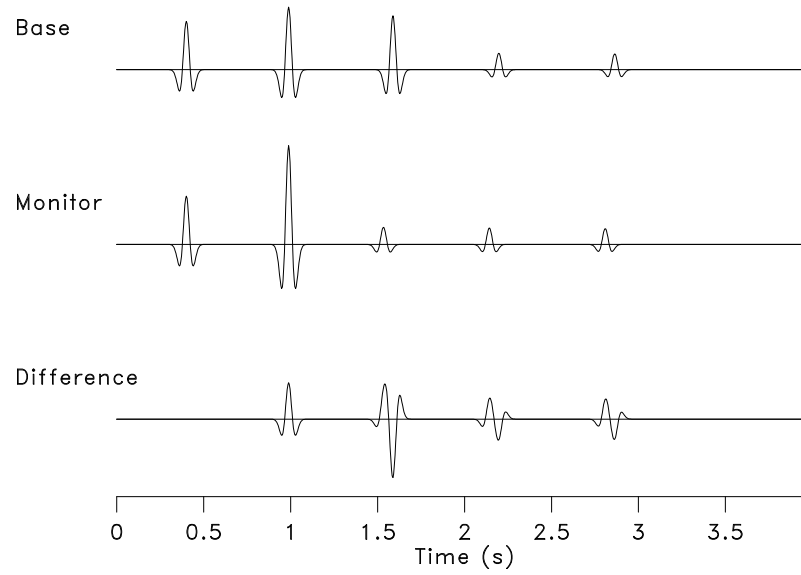


(a)

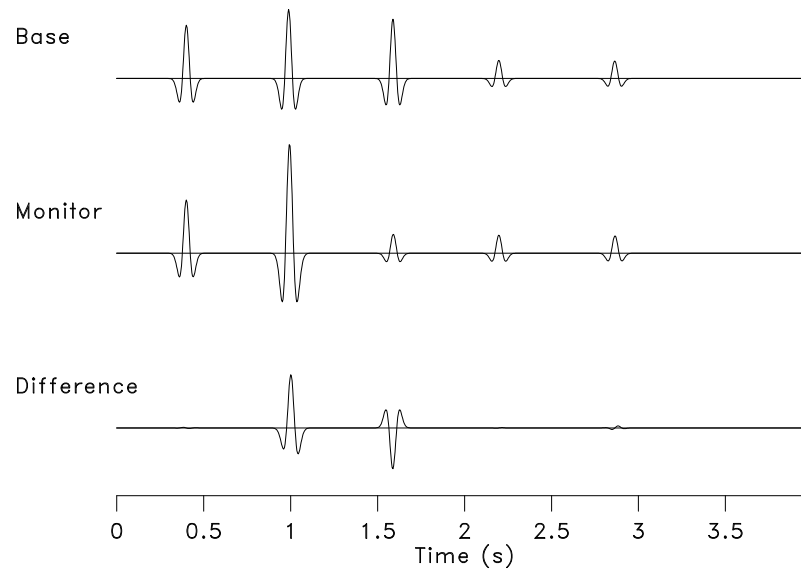


(b)

Figure 1: (a) 1-D synthetic velocity model before (solid line) and after (dashed line) reservoir production. (b) True (solid line) and estimated (dashed line) interval velocity ratio.



(a)



(b)

Figure 2: 1-D synthetic seismic images and the time-lapse difference initially (a) and after image registration (b).

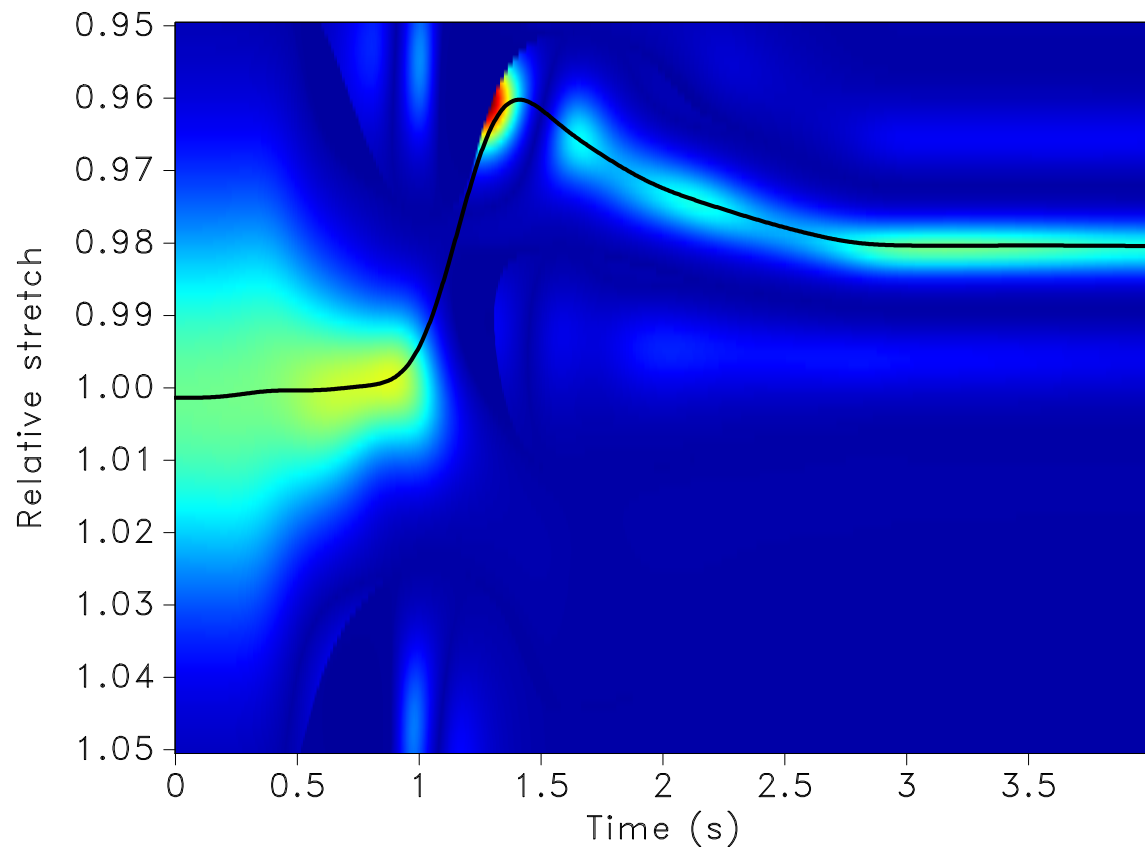


Figure 3: (a) Local similarity scan for detecting the warping function in the 1-D synthetic model. Red colors indicate large similarity. The black curve shows an automatically detected trend.

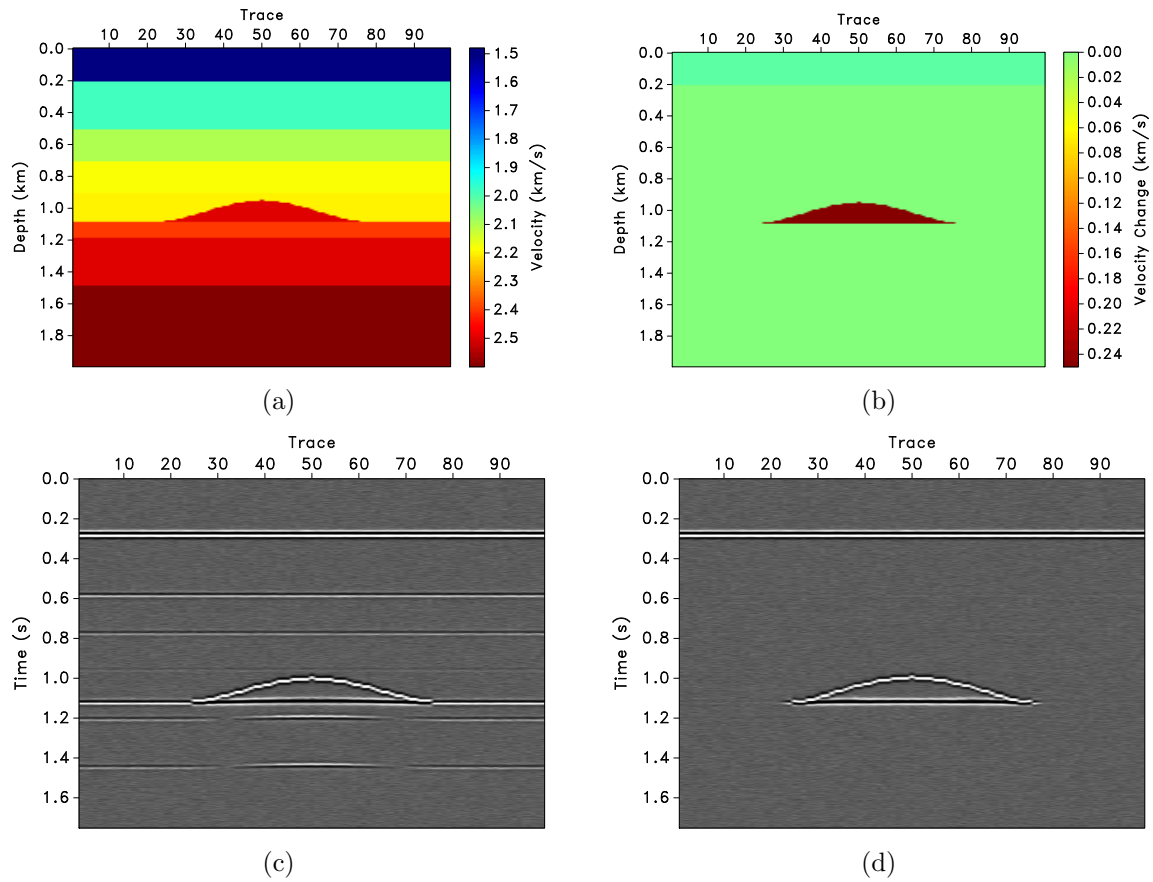


Figure 4: (a) Synthetic model. (b) Time-lapse change containing differences in both the reservoir interval and the shallow overburden. (c) Initial time-lapse difference image. (d) Time-lapse difference image after registration.

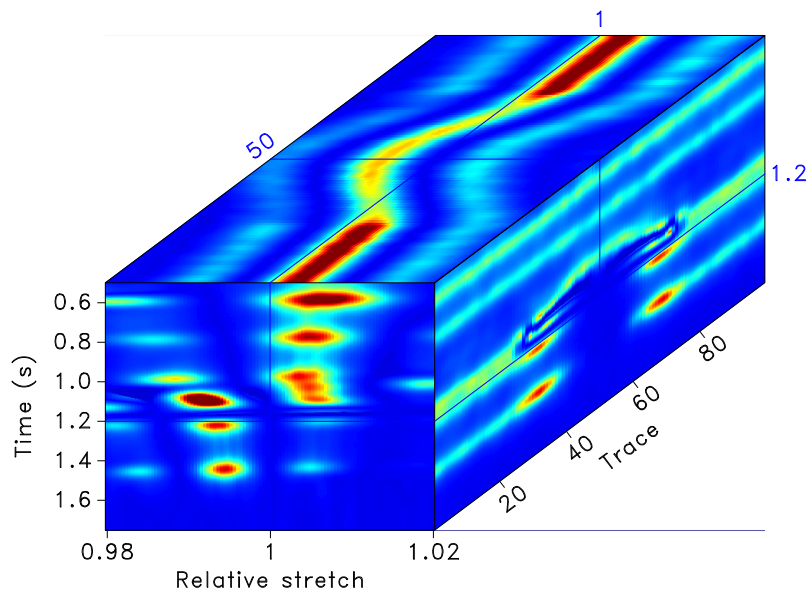


Figure 5: Local similarity scan for the 2-D synthetic model.

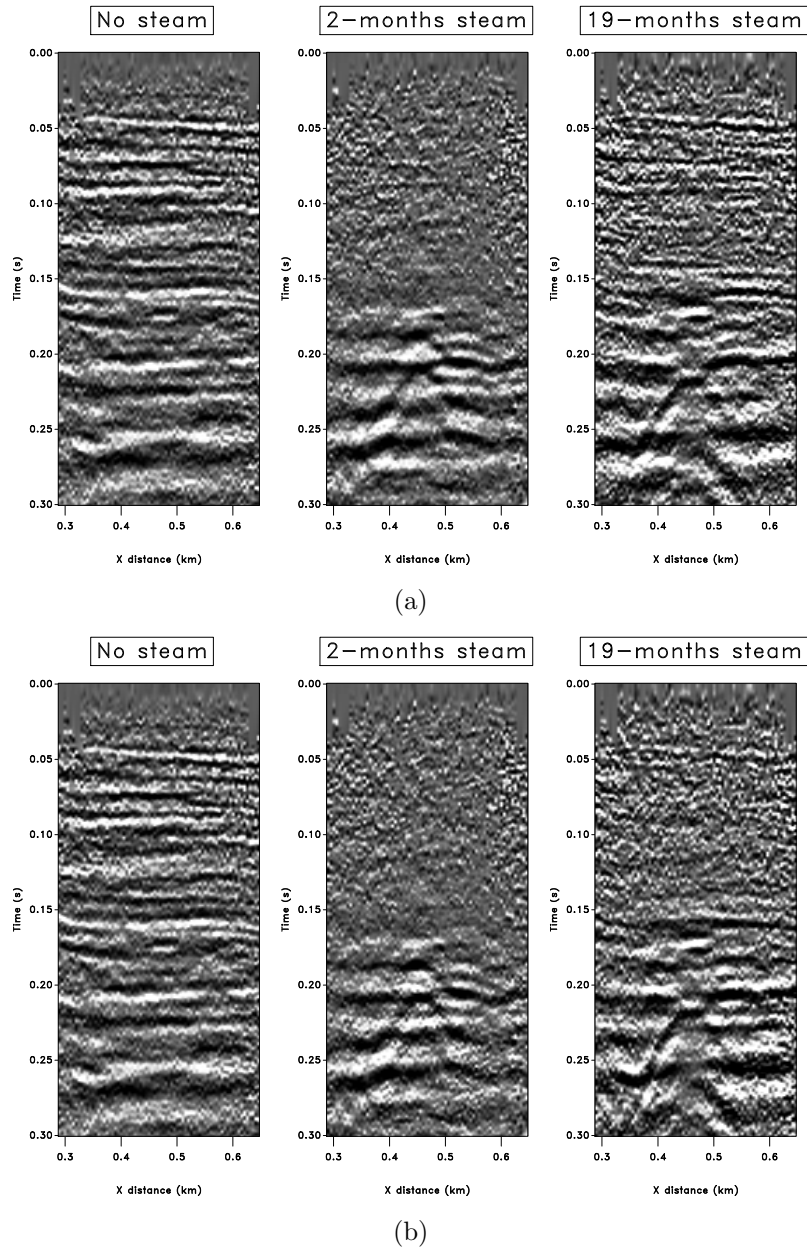


Figure 6: Application to the Duri field data. Base image and time-lapse differences: (a) before registration, reproduced from Lumley (1995a), (b) after registration.

3-D field data

Finally, Figure 6 shows an application of the proposed method to time-lapse images from steam flood monitoring in the Duri field, reproduced from Lumley (1995a,b). Before registration, real differences in the monitor surveys after 2 months and 19 months are obscured by coherent artifacts, which are caused by velocity changes both in the shallow overburden and in the reservoir interval [Figure 6(a)]. Similarly to the results of the synthetic experiments, local-similarity registration succeeds in removing artifact differences both above and below the reservoir level [Figure 6(b)]. After separating the time-shift effect from amplitude changes, one can image the steam front propagation more accurately using time-lapse seismic data. We expect our method to work even better on higher-quality marine data.

CONCLUSIONS

We propose a method of time-lapse image registration based on an application of the local similarity attribute. The local attribute provides a smooth continuous measure of similarity between two images. Perturbing the monitor image by stretching and squeezing it in time while picking its best match to the base image enables an effective registration algorithm. The by-product of this process is an estimate of the time-lapse seismic velocity ratios in the reservoir interval.

Using synthetic and real data examples, we have demonstrated the ability of our method to achieve an accurate time-domain image registration and to remove artifact time-lapse differences caused by velocity changes. Unlike some of the alternative cross-equalization methods, the proposed method is not influenced by amplitude differences and can account for velocity changes in the shallow overburden.

ACKNOWLEDGMENTS

We thank David Lumley for the permission to use results from his Ph.D. thesis. We also thank Aaron Janssen, Brackin Smith, and Ali Tura for inspiring discussions and two anonymous reviewers for helpful suggestions.

This publication is authorized by the Director, Bureau of Economic Geology, The University of Texas at Austin.

REFERENCES

- Aarre, V., 2006, Estimating 4D velocity changes and contact movement on the Norne field: 76th Ann. Internat. Mtg, Soc. of Expl. Geophys., 3115–3119.
- Bertrand, A., S. McQuaid, R. Bobolecki, S. Leiknes, and H. Ro, 2005, A high resolution workflow for 4D-friendly analysis: application to gas-oil contact monitoring at Troll West: 75th Ann. Internat. Mtg, Soc. of Expl. Geophys., 2422–2426.

- Fomel, S., 2007a, Local seismic attributes: *Geophysics*, **72**, A29–A33.
- , 2007b, Shaping regularization in geophysical-estimation problems: *Geophysics*, **72**, R29–R36.
- Fomel, S., M. Backus, K. Fouad, B. Hardage, and G. Winters, 2005, A multistep approach to multicomponent seismic image registration with application to a West Texas carbonate reservoir study: 75th Ann. Internat. Mtg, Soc. of Expl. Geophys., 1018–1021.
- Hale, D., 2006, Fast local cross-correlations of images: 76th Ann. Internat. Mtg, Soc. of Expl. Geophys., 3160–3163.
- Hatchell, P., and S. Bourne, 2005, Rocks under strain: Strain-induced time-lapse time shifts are observed for depleting reservoirs: *The Leading Edge*, **24**, 1222–1225.
- Janssen, A. L., B. A. Smith, and G. W. Byerley, 2006, Measuring velocity sensitivity to production-induced strain at the Ekofisk Field using time-lapse time-shifts and compaction logs: 76th Ann. Internat. Mtg, Soc. of Expl. Geophys., 3200–3203.
- Lumley, D., 1995a, Seismic time-lapse monitoring of subsurface fluid flow: PhD thesis, Stanford University.
- , 2001, Time-lapse seismic reservoir monitoring: *Geophysics*, **66**, 50–53.
- Lumley, D. E., 1995b, 4-D seismic monitoring of an active steamflood: 65th Ann. Internat. Mtg, Soc. of Expl. Geophys., 203–206.
- Modersitzki, J., 2004, Numerical methods for image registration: Oxford University Press.
- Rickett, J., L. Duranti, T. Hudson, and B. Regel, 2007, 4D time strain and the seismic signature of geomechanical compaction at Genesis: *The Leading Edge*, **26**, 644–647.
- Rickett, J., and D. E. Lumley, 2001, Cross-equalization data processing for time-lapse seismic reservoir monitoring: A case study from the Gulf of Mexico: *Geophysics*, **66**, 1015–1025.
- Stucchi, E., A. Mazzotti, and S. Ciuffi, 2005, Seismic preprocessing and amplitude cross-calibration for a time-lapse amplitude study on seismic data from the Oseberg reservoir: *Geophysical Prospecting*, **53**, 265–282.
- Tura, A., T. Barker, P. Cattermole, C. Collins, J. Davis, P. Hatchell, K. Koster, P. Schutjens, and P. Wills, 2005, Monitoring primary depletion reservoirs using amplitudes and time shifts from high-repeat seismic surveys: *The Leading Edge*, **24**, 1214–1221.